Biochemistry and Biophysics Reports 33 (2023) 101430

Contents lists available at ScienceDirect

Biochemistry and Biophysics Reports

journal homepage: www.elsevier.com/locate/bbrep

Combined treatments with AZD5363, AZD8542, curcumin or resveratrol induce death of human glioblastoma cells by suppressing the PI3K/AKT and SHH signaling pathways

Rosalinda Mejía-Rodríguez [a], Daniel Romero-Trejo [a], Rosa O. González [b,1], José Segovia [a,*]

[a] Departamento de Fisiología, Biofísica y Neurociencias, Centro de Investigación y de Estudios Avanzados del IPN, Mexico
[b] Departamento de Matemáticas, Universidad Autónoma Metropolitana-Iztapalapa (UAM-I), Mexico

ARTICLE INFO

Keywords:
Glioma
Combined therapy
Resveratrol
Curcumin
AZD5363
AZD8542

ABSTRACT

Glioblastoma (GBM) is a very aggressive tumor that presents vascularization, necrosis and is resistant to chemotherapy and radiotherapy. Current treatments are not effective eradicating GBM, thus, there is an urgent need to develop novel therapeutic strategies against GBM. AZD5363, AZD8542, curcumin and resveratrol, are widely studied for the treatment of cancer and in the present study we explored the effects of the administration of combined treatments with AZD5363, AZD8542, curcumin or resveratrol on human GBM cells. We found that the combined treatments with AZD5363+AZD8542+Curcumin and AZD8542+Curcumin+Resveratrol inhibit the PI3K/AKT and SHH survival pathways by decreasing the activity of AKT, the reduction of the expression of SMO, pP70S6k, pS6k, GLI1, p21 and p27, and the activation of caspase-3 as a marker of apoptosis. These results provide evidence that the combined treatments AZD5363+AZD8542+Curcumin and AZD8542+Curcumin+Resveratrol have the potential to be an interesting option against GBM.

1. Introduction

Glioblastoma (GBM) is the most malignant primary brain tumor with a very poor prognosis [1–3]. Despite advances in surgical, radiation, and chemotherapy techniques, patients have a median overall survival of approximately 15 months [2,4].

The pathogenic processes underlying GBM include the dysregulation of different signaling pathways which are interconnected and involved in the inactivation of proapoptotic genes and cell cycle regulator genes, as well as the amplification and/or hyper-activation of oncogenes implicated in the growth, survival, angiogenesis, migration and resistance to chemotherapy and radiotherapy of cancer cells [5–8].

A frequently dysregulated signaling pathway in glioma is PI3K/AKT/mTOR, this pathway is associated with higher tumor grade, decreased levels of apoptosis, reduced patient survival and radiation resistance [9–11].

The Sonic Hedgehog Signaling (SHH) pathway is also involved in GBM pathogenesis. SHH is associated with the origin, progression of the tumor, inhibition of apoptosis and cancer stem cell self-renewal of different tumors, including glioma [12,13].

We decided it would be relevant to further investigate the effects of combined pharmacological treatments inhibiting the activity of cellular signaling pathways frequently altered in GBM, in particular PI3K/AKT and SHH as a potential strategy for the treatment of GBM. For this work, we selected four agents (AZD5363, AZD8542, Curcumin and Resveratrol) that inhibit these pathways, and determined their effects, when applied independently or in combinations, on GBM growth and eliminating cancer cells.

AZD5363 or Capivasertib (AstraZeneca) is a pan-AKT kinase inhibitor that has been tested both *in vitro* and *in vivo*, it is an ATP-competitive catalytic inhibitor, that prevents substrate phosphorylation by AKT [14]. Additionally, AZD5363 crosses the blood-brain barrier, and it has demonstrated efficacy in a mouse xenograft meningioma model [15].

AZD8542 (AstraZeneca) is a SMO inhibitor also tested *in vitro* and *in vivo*, it inhibits the expression of GLI in a human prostate stromal cell line and *in vivo* inhibited tumor growth of tumor xenografts of pancreatic and colon cancer [16].

Curcumin (CCR) is a yellow polyphenolic compound, extracted from

* Corresponding author. Departamento de Fisiología, Biofísica y Neurociencias, Centro de Investigación y de Estudios Avanzados del IPN, Av. IPN # 2508, 07300, Mexico.
E-mail address: jsegovia@fisio.cinvestav.mx (J. Segovia).
[1] Deceased.

https://doi.org/10.1016/j.bbrep.2023.101430
Received 31 October 2022; Received in revised form 2 January 2023; Accepted 16 January 2023

the root of the *curcuma longa* plant native to Asia, and the Food and Drug Administration (FDA) has approved CCR as "generally recognized as safe" (GRAS) [17]. CCR decreases cell proliferation, migration and induces apoptosis in multiple human carcinomas including neuroblastoma, lung cancer, prostate cancer, breast cancer and GBM [18–24]. Particularly, CCR downregulates both mRNA and protein levels of molecules involved in the SHH-GLI pathway in human GBM cells [19,25] moreover, it also decreases the activation of the PI3K/AKT survival pathway in human GBM cells [22,26]. Furthermore, CCR crosses the blood-brain barrier and is harmless to normal mice brain cells both *in vivo* and *in vitro* [18,22]. Nevertheless, CCR has characteristics that affect its study and functional analysis, including: low solubility in water at room temperature and at neutral pH and therefore high propensity to aggregate [27], poor absorption and distribution in the organism possibly due to low cell permeability [28], CCR is photoreactive so it is easily degraded [29], and the CCR wavelength may interfere with fluorescence-based bioassays [28].

Resveratrol (RV) is a natural polyphenol found in many plants and fruits including peanuts, blackberries, blueberries and grapes. RV is a phytoalexin, an antimicrobial compound, which accumulates in some plants [30,31]. It has been shown both *in vitro* and *in vivo* that RV promotes apoptosis, regulates cell cycle and decreases cell proliferation and migration of cancer cells [32–36]. Particularly, RV reduces AKT phosphorylation and induces the activation of p53 in human GBM cells [35] moreover, it also inhibits the SHH signaling pathway by decreasing the levels of GLI in different cancers including prostate and gastric cancer [37,38]. Furthermore, RV crosses the blood-brain barrier and exerts protective effects against cerebral ischemic injury [39]. However, limitations of RV for scientific research are its poor solubility in water, chemical instability, poor tissue absorption [40,41] and different dose-dependent effects [41].

For the present work we used combined treatments with AZD5363, AZD8542, CCR and RV against GBM *in vitro*. We demonstrated that the combined administration of AZD5363+AZD8542+CCR or AZD854 2+CCR+RV have anticancer effects *in vitro*, through the inhibition of the PI3K/AKT and SHH survival pathways, the regulation of p21 and p27 and inducing apoptosis through the activation of caspase-3 on U-87 MG and A172 human GBM cell lines. We suggest that the simultaneous targeting of the PI3K/AKT/SHH pathways is a potentially relevant adjuvant for the treatment of GBM.

2. Materials and methods

2.1. Cell culture

U-87 MG human GBM cells (passages four through fourteen) were obtained from the American Type Culture Collection (Manassas, VA, USA). Cells were cultured in DMEM-HG (Dulbecco's Modified Eagle Medium High-Glucose) (Gibco by Life Technologies, cat. 12800–017) supplemented with 10% fetal bovine serum (Gibco by Life Technologies, cat. 16000–044), 1% L-glutamine (Sigma-Aldrich, cat.G8540), 100 U/mL of Penicillin and 100 μg/mL of Streptomycin (Gibco by Life Technologies, cat. 15140–122), and maintained at 37 °C in a 95% air, 5% CO_2 atmosphere. A172 human GBM cells (passages two through fourteen) were kindly provided by Dr. Benjamín Pineda Olvera (National Institute of Neurology and Neurosurgery, Mexico City); SH-SY5Y human neuroblastoma cells (passages six through fourteen) were obtained from the American Type Culture Collection (Manassas, VA, USA). Both A172 and SH-SY5Y cells were cultured in DMEM-F12 (Dulbecco's Modified Eagle Medium Ham's Nutrient Mixture F12) (Gibco by Life Technologies, cat. 12500–062) supplemented with 10% fetal bovine serum (Gibco by Life Technologies, cat. 16000–044), 1% L-glutamine (Sigma-Aldrich, cat.G8540), 100 U/mL of Penicillin and 100 μg/mL of Streptomycin (Gibco by Life Technologies, cat. 15140–122), and maintained at 37 °C in a 95% air, 5% CO_2 atmosphere.

2.2. Gliomaspheres culture

Briefly, gliomaspheres were generated as previously described [42–44]. U-87 MG and A172 human GBM cells were cultured in serum-free DMEM supplemented with 2% B27 (Gibco by Life Technologies, cat. 12587010), 20 ng/ml epidermal growth factor (EGF) (Sigma-Aldrich, cat. H9644) and 20 ng/ml basic fibroblast growth factor (bFGF) (Gold Biotechnology, cat. 1140-02-100) and maintained at 37 °C in a 95% air, 5% CO_2 atmosphere. After 24 h, floating cells were re-seeded in a new 60 mm culture plate, in supplemented serum-free medium and the medium was changed every 2 days. Floating aggregates, known as gliomaspheres were formed within 3–5 days after seeding. For morphological examination, pictures were taken with a Nikon TMS inverted microscope.

2.3. Therapeutic agents

AZD5363 and AZD8542 (generously provided by AstraZeneca), CCR (Sigma-Aldrich, cat. C1386) and RV (Sigma-Aldrich, cat. R5010) were dissolved in dimethyl sulfoxide (DMSO). For cytotoxicity assays, stock solutions were used at 10 mmol/L (AZD5363 and AZD8542) and 20 mmol/L (CCR and RV), subsequently, were diluted in DMEM-HG and DMEM-F12 medium, corresponding to each cell line. The solutions of the combined treatments were used at the corresponding IC50 concentrations for each agent. All solutions were stored at −20 °C.

2.4. MTT assay

The U-87 MG and A172 cells were seeded in 48-well plates (15,000 cells/well). For cytotoxicity assays the cells were incubated with increasing concentrations of AZD5363, AZD8542, CCR or RV. To determine the effect of combined therapies on cell viability cells were exposed to eleven different combinations with AZD5363, AZD8542, CCR or RV. After 72 h, viable cells were assessed by measuring the conversion of the 3-(4,5- dimethylthiazol-2-yl)-2,5-diphenyltetrazolium bromide (MTT) dye (Sigma-Aldrich, cat. M2128) (5 mg/ml) into formazan, for 2 h. Next, the crystals were dissolved with DMSO. The absorbance of the reaction was determined using an automated microplate reader (Bio-Rad).

2.5. Reverse transcription-polymerase chain reaction analysis

Total RNA extraction was performed using the TRIzol Reagent (Invitrogen, cat. #15596026, USA), according to the manufacturer's instructions. Subsequently, 5 μg of RNA was treated with DNAse (New England BioLabs, cat. #M0303S) and converted to cDNA using MMLV reverse transcriptase (Invitrogen, cat. #28025013) to perform the PCR [45]. To amplify AKT mRNA, the following primers were used: forward 5′-GCCATGAAGATCCTCAAGAAGG-3′ and reverse 5′-CATCATCTCG TACATGACCACG-3′. To amplify SMO mRNA, the following primers were used: forward 5′-CCCAGTTCATGGATGGTGC-3′ and reverse 5′-GTGGTTGCTCTTGATGGAGAAC-3′. To amplify β-actin mRNA, the following primers were used: forward 5′-TGGCACCACACCTTCTACA-3′ and reverse 5′-TCACGCACGATTTCCC-3′ [46].

2.6. Colony formation assay

Cells were seeded in 60 mm cell culture dishes at a density of 300,000 cells/dish and allowed to grow for 24 h. Then, cells were incubated in the absence or in the presence of the various combined treatments for another 24 h. Subsequently, cells were re-plated in new 60 mm cell culture dishes at a density of 300 cells/dish with fresh medium to assess their clonogenic ability. Cells were cultured for an additional 10 days in complete medium. The colonies obtained were washed with PBS, fixed and stained with 0.1% crystal violet in ethanol. A colony contains at least 50 cells.

2.7. Proliferation assay

Cell proliferation was detected using the EdU (5-ethynyl-2-deoxyuridine) incorporation assay according to the manufacturer's protocol (Click-iTEdU imaging kit, Invitrogen, cat. C10337). Briefly, cells were incubated with 20 μM of EdU for 4 h. EdU was incorporated into DNA during active DNA synthesis and was detected with a click reaction, a copper-catalyzed covalent reaction between azide/alkyne [47]. Cell nuclei were counterstained with Vectashield Antifade Mounting Medium with DAPI (Vector Laboratories, cat. H-2000-2). Images were obtained with a 40x objective using a Leica TCS SP8 confocal microscope and processed with the Image J software (National Institutes of Health, USA).

2.8. Western blot assays

Protein extraction was performed using a lysis buffer containing a protease inhibitor cocktail (Complete Roche Diagnostics, cat. 11836170001). Samples containing 50 μg of total protein per condition, were separated in either 8% or 10% SDS-PAGE gels and transferred onto the polyvinylidene-difluoride (PVDF) membranes [48] (Bio-Rad, cat. #1620177), which were subsequently blocked for 1 h at room temperature with a solution of 3% non-fat milk in Tris buffered saline (TBS) 1% and then incubated overnight at 4 °C with primary antibodies against p21 (Cell Signaling, USA; cat. 2947T, dilution 1:1000), p27 (Santa Cruz Biotechnology, USA; cat. sc1641, dilution 1:200), Cyclin-D1 (Biorbyt, USA; cat. orb10496, dilution 1:1000), Caspase-3 (Cell Signaling, USA; cat. 9662S, dilution 1:500), *p*-AKT (Ser-473) (Cell Signaling, USA; cat. 4060S, dilution 1:1000), *t*-AKT (Cell Signaling, USA; cat. 4691S, dilution 1:5000) p-p70 S6k (Santa Cruz Biotechnology, USA; cat. sc-8416, dilution 1:1000), p-S6 (Cell Signaling, USA; cat. 4858S, dilution 1:1000), SMO (Abcam, UK; Cat. ab113438, dilution 1:200), GLI1 (Cell Signaling, USA; Cat. C68H3, dilution 1:500) and β-actin (Sigma Aldrich, USA; Cat. A3854, dilution 1:80,000). Blots were washed and incubated for 1 h at room temperature with HRP-Goat anti-mouse antibody (Invitrogen, Camarillo, CA; Cat. 62–6520, dilution 1:10,000) or HRP-Goat anti--rabbit (Invitrogen, Camarillo, CA; Cat. 62–6120, dilution 1:20,000). Proteins were revealed by chemiluminescence (PerkinElmer Inc., Waltham, MA, USA, cat. NEL104001EA). Images were captured with a FUSION solo S (Vilber) instrument and the densitometry analyses performed using the Image J software (National Institutes of Health, USA).

2.9. Statistical analysis

For cytotoxicity, cellular viability, colony formation, proliferation and protein levels determined by Western blot analysis, we used one-way ANOVA followed by Tukey's or Games Howell multiple comparison test. We used the GraphPad Prism 6 software. All values are means ± SEM. Statistical significance is indicated as: *$p < 0.05$, **$p < 0.01$, ***$p < 0.001$, ****$p < 0.0001$. ns, non-significant.

3. Results

3.1. AZD5363, AZD8542, CCR and RV have cytotoxic effects on human GBM cells

Employing RT-PCR we demonstrated that both the human glioma-derived U-87 MG and A-172 cell lines express both AKT and SMO, critical components (Fig. 1A), of the PI3K/AKT and SHH signaling pathways [9–13,49–52] and important molecular targets of AZD5363, AZD8542, CCR and RV [14,16,19,22,25,26,35,37,38]. Thus, both the U-87 MG and A-172 cell lines are good models to evaluate the effect of treatments with different combinations of AZD5363, AZD8542, CCR and RV against GBM. When the U-87 MG and A-172 cell lines were incubated

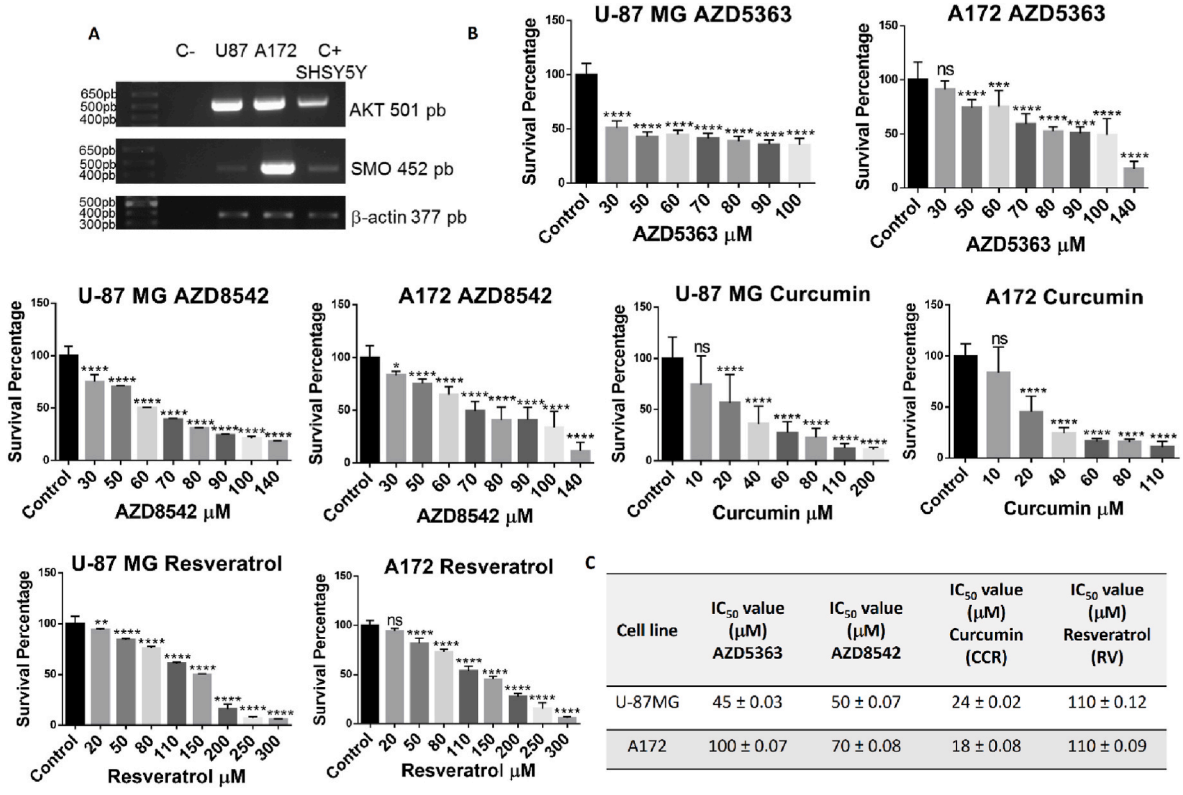

Cell line	IC_{50} value (μM) AZD5363	IC_{50} value (μM) AZD8542	IC_{50} value (μM) Curcumin (CCR)	IC_{50} value (μM) Resveratrol (RV)
U-87MG	45 ± 0.03	50 ± 0.07	24 ± 0.02	110 ± 0.12
A172	100 ± 0.07	70 ± 0.08	18 ± 0.08	110 ± 0.09

Fig. 1. Molecular characterization and cytotoxic effects of AZD5363, AZD8542, CCR and RV in human GBM cells. (**A**) RT-PCR products for AKT (501 bp), SMO (452 pb) and β-actin (377 pb), SH-SY5Y neuroblastoma cells were used as positive controls. (**B**) Cytotoxic effect of AZD5363, AZD8542, CCR and RV on U-87 MG and A172 cell lines as assessed by the MTT assay. Bars are means ± SEM of three independent experiments. One-way ANOVA, followed by Tukey's, *$p < 0.05$, **$p < 0.01$, ***$p < 0.001$, ****$p < 0.0001$. ns, non-significant. (**C**) IC50 values of AZD5363, AZD8542, CCR and RV for the U-87 MG and A172 cell lines.

with increasing concentrations of AZD5363, AZD8542, CCR and RV, we observed, employing the MTT assay, a dose-dependent cytotoxic effect (Fig. 1B). The sensitivity to AZD5363 and AZD8542 between the two cell lines was different, whereas for CCR and RV was similar. Using the GraphPad Prism 6 software, we analyzed the cytotoxicity data from the cells lines to obtain the IC50 of each agent (Fig. 1C). The IC50 of U-87 MG for AZD5363 is 45 μM, for AZD8542 is 50 μM, for CCR is 24 μM and for RV is 110 μM. The IC50 of A172 for AZD5363 is 100 μM, for AZD8542 is 70 μM, for CCR is 18 μM and for RV is 110 μM. CCR has the lowest IC50 values in both cell lines, which suggests it is the most potent agent. For the subsequently studies we used the IC50 values of each anticancer agent for each cell line.

3.2. The combined administration of AZD5363, AZD8542, CCR and RV is more effective than monotherapy

The balance between cell proliferation and cell death is regulated by signaling pathways that are interconnected. When this balance is dysregulated cancer may be favored, therefore it is important to find targeted therapies against the aberrant proteins that alter the functioning of signaling pathways [53]. Since the combination of anticancer agents for specific molecular targets enhances efficacy compared to monotherapy [54,55], we examined the cell viability of the combined administration of AZD5363, AZD8542, CCR and RV using the IC50 values previously determined in the human GBM cell lines U-87 MG and A172 (Fig. 1C). Cells were exposed to 11 combinations of the four agents for 72 h. Using the MTT assay, we observed that all eleven combinations induced more than 50% cell death of U-87 MG and A172 cells (Fig. 2A). These results demonstrate that all the combined treatments are more efficacious inducing cell death, than when each agent is independently used. The combinations inducing the lower levels of survival for the U-87 MG cell line were AZD5363+AZD8542+CCR, AZD5363+AZD8542+RV+CCR, AZD5363+AZD8542+RV and AZD8542+CCR+RV (Fig. 2B). The best combinations with the lower viability for the A172 cell line were AZD5363+CCR+RV, AZD5363+AZD8542+RV, AZD8542+CCR+RV and AZD5363+AZD8542+CCR (Fig. 2B). Based on statistical analysis, for the subsequent analysis we continued only with the following combinations: AZD5363+AZD8542+RV, AZD8542+CCR+RV and ZD5363+AZD8542+CCR (Fig. 2B), which are the combinations with the lowest viability in both cell lines.

3.3. The combined treatments with AZD5363+AZD8542+CCR or AZD8542+CCR+RV inhibit the formation of colonies derived from human glioblastoma cells

Conventional treatments for GBM include surgical resection followed by radiotherapy and/or chemotherapy, however, recurrence rate is greater than 90% [56]. GBM recurrence is defined as tumor progression starting from residual cancer cells after standard treatment and these tumors tend to be more aggressive and resistant to therapy than the

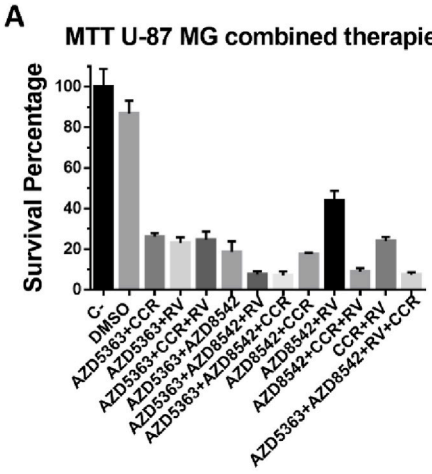

U-87 MG					
Combined therapies	1	2	3	4	5
AZD5363+AZD8542+CCR	**7.14**				
AZD5363+AZD8542+RV+CCR	7.46				
AZD5363+AZD8542+RV	**7.54**				
AZD8542+CCR+RV	**8.92**				
AZD8542+CCR		17.5			
AZD5363+AZD8542		18.6	18.6		
AZD5363+RV		23.1	23.1		
CCR+RV		24.1	24.1		
AZD5363+CCR+RV		24.6	24.6		
AZD5363+CCR			26.1		
AZD8542+RV				43.8	
DMSO					86.8
C-					100

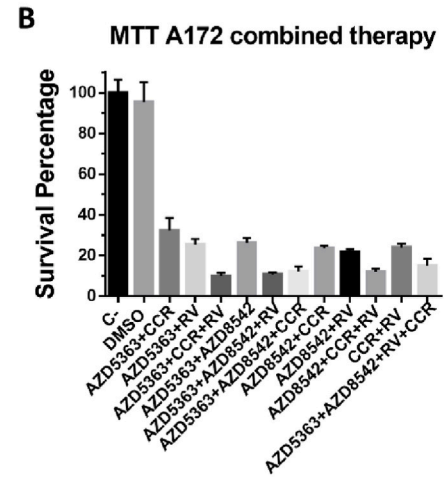

A172					
Combined therapies	1	2	3	4	5
AZD5363+CCR+RV	9.94				
AZD5363+AZD8542+RV	**10.9**				
AZD8542+CCR+RV	**12**				
AZD5363+AZD8542+CCR	**12.2**				
AZD5363+AZD8542+RV+CCR	15	15			
AZD8542+RV		21.8	21.8		
AZD8542+CCR			23.7		
CCR+RV			24.1		
AZD5363+RV			25.5	25.5	
AZD5363+AZD8542			26.3	26.3	
AZD5363+CCR				32.4	
DMSO					95.5
C-					100

Fig. 2. Effects of the combinations of the four agents in human GBM cells. U-87 MG and A172 cells were treated with the indicated combinations of AZD5363, AZD8542, CCR and RV. After 72 h of treatments cell viability was determined by the MTT assay. Fresh medium and DMSO were used as negative control. (**A**) Left panel, shows survival (as percentage) of U-87 MG cells; the right panel shows the statistical analysis. (**B**) Left panel, shows survival (as percentage) of A172 cells; the right panel shows the statistical analysis. Bars are means ± SEM of three independent experiments. One-way ANOVA, followed by Games Howell, *$p < 0.05$.

original [56]. For this reason it is very important to find efficacious long-term therapies that prevent the growth of residual cancer cells. To determine the efficacy of the combined therapies with AZD5363+AZD8542+RV, AZD8542+CCR+RV or AZD5363+AZD8542+CCR and assess whether they may have a prolonged effect we used *in vitro* colony formation or clonogenic cell assays to determine if a single cancer cell can recover after a potentially lethal damage and evaluate its ability to proliferate and create a new colony, consisting in at least 50 cells [57]. We observed that the U-87 MG cell line forms dispersed colonies in comparison with the A172 cell line, which forms agglomerate colonies (Fig. 3A). Fig. 3B show that, as expected, control cells grow and form colonies from both cell lines. Moreover, we observed that cells form colonies when incubated in the presence of AZD5363+ADZ8542+RV when compared with the AZD5363+AZD8542+CCR and AZD8542+CCR+RV, which do not form colonies.

This indicates that the AZD5363+ADZ8542+RV combination allows residual cancer cell growth that would likely permit long-term recurrence. There are fewer colonies from A172 cells when treated with the AZD5363+ADZ8542+RV combination compared with its effect in the U-87 MG cell line, however sufficient colonies are formed that could trigger recurrence (Fig. 3C). Based on these data, we decided that for the subsequent experiments, we would only use the combinations that did not generate long-term colonies.

3.4. The administration of the AZD5363+AZD8542+CCR or AZD8542+CCR+RV combinations inhibits the proliferation of human GBM cells and decreases the survival of gliomaspheres

To determine the time course of death of cells treated with the different combinations that inhibit the formation of colonies, the U-87 MG and A172 cell lines were exposed to AZD5363+AZD8542+CCR or AZD8542+CCR+RV for 24, 48 and 72 h, and then cell viability was determined using the MTT assay. We observed that 24 h after the treatments there is approximately 50% survival of both cell lines whereas, after 48 h of treatment there is a more marked growth inhibition of GBM cells compared with control cells (Fig. 4A). Hence, we next asked the fate of cells alive at 24 h of treatment, and determined their proliferation rate as assessed by the EdU incorporation assay. Our results show that 24 h after cell exposure to AZD5363+AZD8542+CCR or AZD8542+CCR+RV there is a drastic reduction of EdU positive cells compared with control cells, from both the U-87 MG and the A172 cell lines. This means the percentage of cells that survive 24 h of treatment with AZD5363+AZD8542+CCR or AZD8542+CCR+RV halt proliferating, indicating that the cells will likely no longer recover. After these treatments the human GBM cells acquired permanent damage that will lead to death. (Fig. 4B). Additionally, using the MTT assay, we determined that the combined treatments with AZD5363+AZD8542+CCR or AZD8542+CCR+RV significantly decreased the viability of gliomaspheres derived from both U-87 MG and A172 cell lines (Fig. 4C). Taken together the present results indicate that the combined treatments with AZD5363+AZD8542+CCR or AZD8542+CCR+RV could be a good strategy for the treatment of GBM.

3.5. The administration of the AZD5363+AZD8542+CCR or AZD8542+CCR+RV combinations inhibits the PI3K/AKT and SHH survival pathways on human GBM cells

The activation of the PI3K/AKT and SHH pathways is associated with

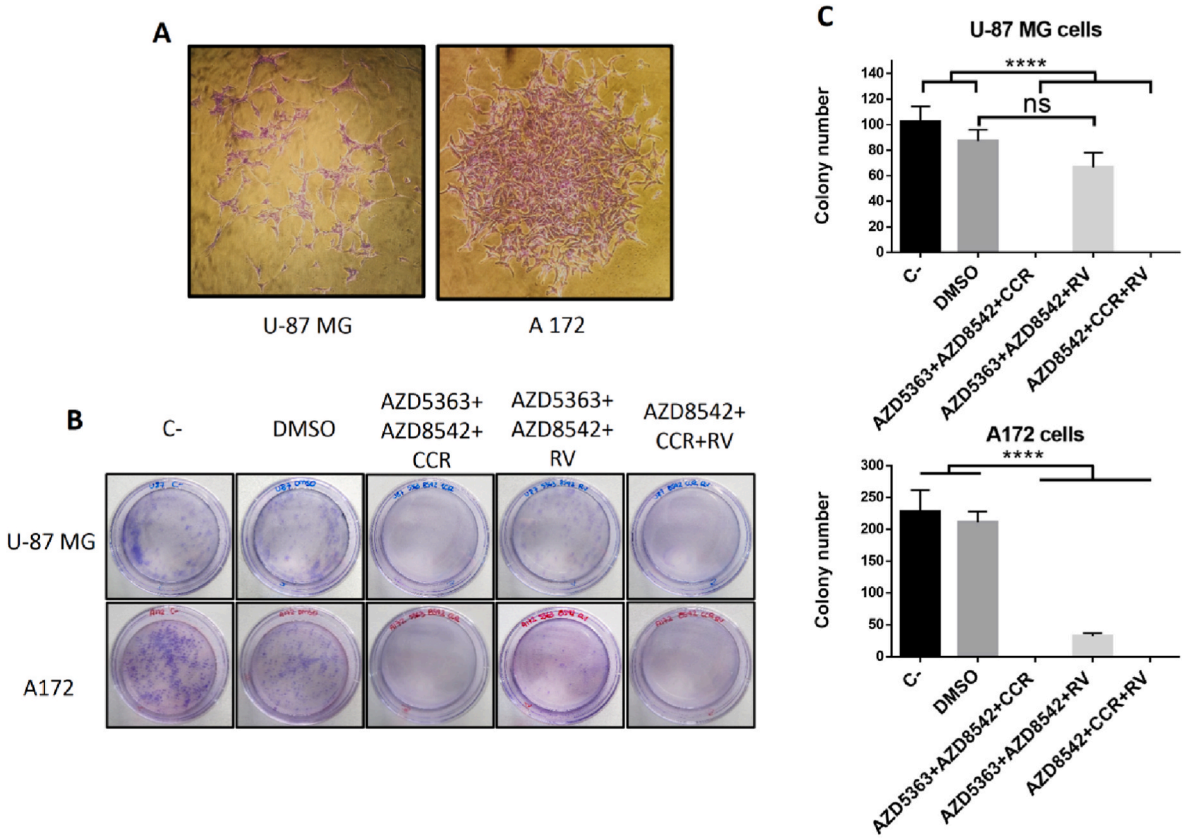

Fig. 3. Clonogenic analysis of the AZD5363+AZD8542+RV AZD5363+AZD8542+CCR and AZD8542+CCR+RV effects on human GBM long-term survival. (**A**) Representative images from colonies obtained from control U-87 MG (left panel) and A172 (right panel) cells, respectively. (**B**) Representative image of dishes with stained colonies obtained from U-87 MG (upper panel) and A172 (lower panel) treated cells. (**C**) Quantitative analysis of colony formation from U-87 MG (upper panel) and A172 (lower panel) treated cells. Bars are means ± SEM of three independent experiments. One-way ANOVA, followed by Tukey; $^{**}p < 0.01$, $^{****}p < 0.0001$. ns, non-significant.

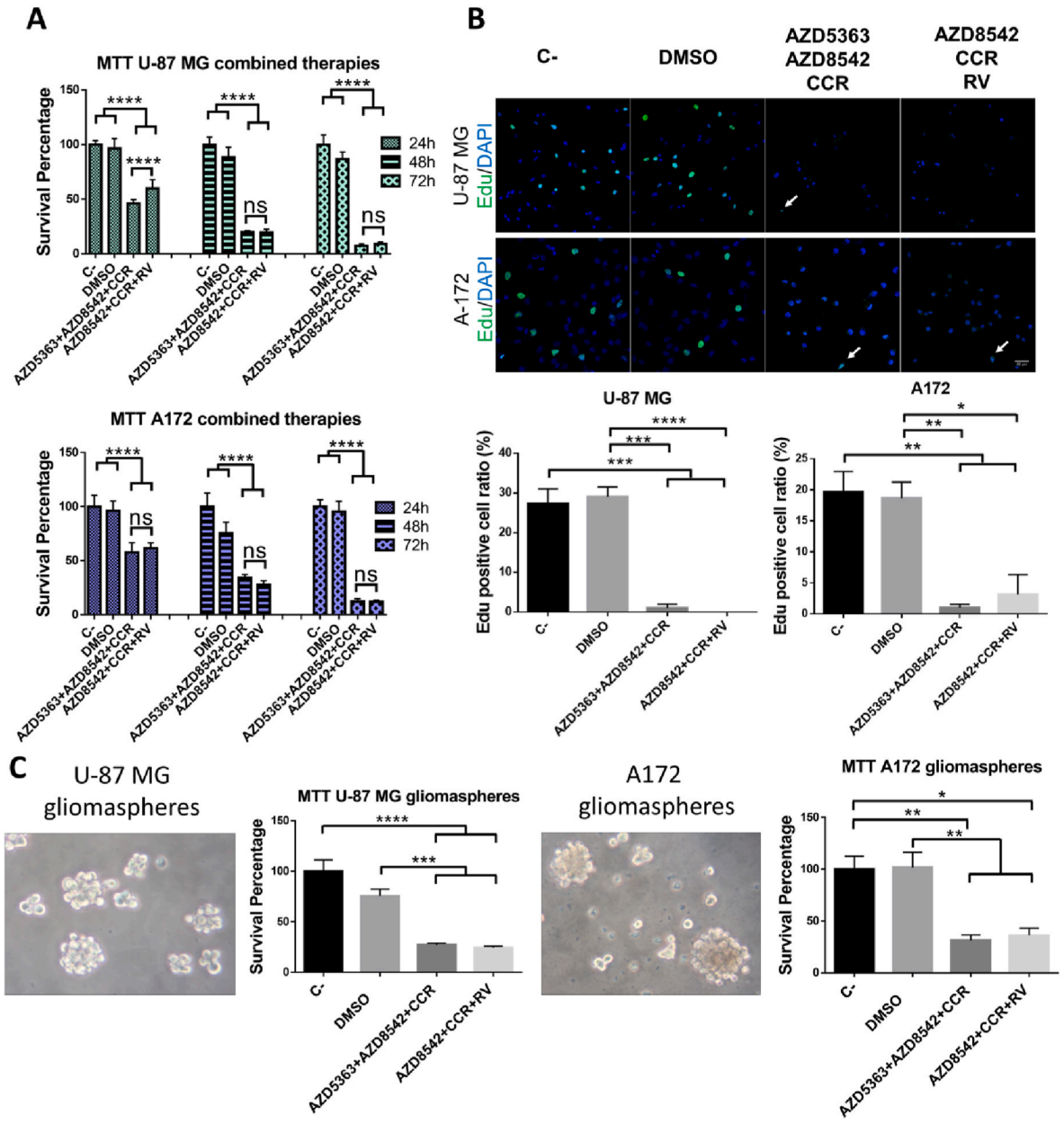

Fig. 4. Determination of the effect of the combined treatments of AZD5363+AZD8542+CCR or AZD8542+CCR+RV against GBM recurrence. (A) Graphs show survival (as percentage) of U-87 MG (upper panel) and A172 (lower panel), cell lines incubated with AZD5363+AZD8542+CCR or AZD8542+CCR+RV for 24 h, 48 h and 72 h; cell viability was determined by MTT. (B) Left panel shows a representative image of EdU positive cells, U-87 MG (upper panel) and A172 (lower panel) cells, bar 40 μm. Green cells, are EdU positive cells, arrows, indicate positive cells treated with AZD5363+AZD8542+CCR or AZD8542+CCR+RV. Right panel shows the percentage of EdU positive cell ratio, U-87 MG (left panel) and A172 (right panel) cell lines. Data obtained from three fields per experimental condition, of three independent experiments. Percentage of positive EdU cells was obtained: EdU+/DAPI+ * 100%. (C) A representative image showing U-87 MG gliomaspheres (left panel) and A172 gliomaspheres (right panel). Graphs, shows the survival of U-87 MG cells, derived gliomaspheres (as percentage) and of A172 cells derived gliomaspheres (as percentage), treated with AZD5363+AZD8542+CCR and AZD8542+CCR+RV for 72 h. One-way ANOVA, followed by Tukey; *$p < 0.05$, **$p < 0.01$, ***$p < 0.001$, ****$p < 0.0001$. ns, non-significant. (For interpretation of the references to colour in this figure legend, the reader is referred to the Web version of this article.)

increasing tumor grade, cell proliferation, survival, invasion, angiogenesis and decreased levels of apoptosis in human gliomas [8,9,49]. Moreover, the PI3K/AKT and SHH signaling pathways synergize to maintain cell proliferation and favor GBM aggressiveness [58,59]. To evaluate the molecular mechanism underlying the effect of 48 h of incubation with AZD5363+AZD8542+CCR or AZD8542+CCR+RV on cell viability, we determined the activity of the previously mentioned signaling pathways. We observed, by Western blot analysis, that the levels of both pAKT and tAKT decrease in the U-87 MG cell line with the two combined treatments. Similarly the levels of pAKT and tAKT diminished in the A172 cells line with combined administration of AZD8542+CCR+RV, whereas the levels pAKT increased in the A172 cell line receiving AZD5363+AZD8542+CCR. It is noteworthy, that in these experiments the densitometry analysis were normalized to β-actin, because we observed an unexpected decrease of total AKT on both U-87 MG and A172 cell lines (Fig. 5B and D). On the other hand, when we performed the densitometry analysis normalizing pAKT/tAKT, we observed that most of the AKT protein is phosphorylated, since its levels

were either maintained or increased with respect to the controls (Fig. Sup. 1). Despite the fact that most of the AKT protein is phosphorylated, we observed a decrease in the expression of p-p70 S6k and pS6k proteins, which are crucial effectors of the PI3K/AKT signaling pathway. On the other hand, the combined treatments with AZD5363+AZD8542+CCR or AZD8542+CCR+RV induced a significant decrease in the activities of SMO and GLI1 both in U-87 MG and A172 cell lines. Taken together, these results indicate that the treatments with the AZD5363+AZD8542+CCR or AZD8542+CCR+RV combinations inhibit the PI3K/AKT and SHH signaling pathways and thus impede the synergy between the two pathways in both cell lines, thus contributing to achieve a long-term anticancer effect.

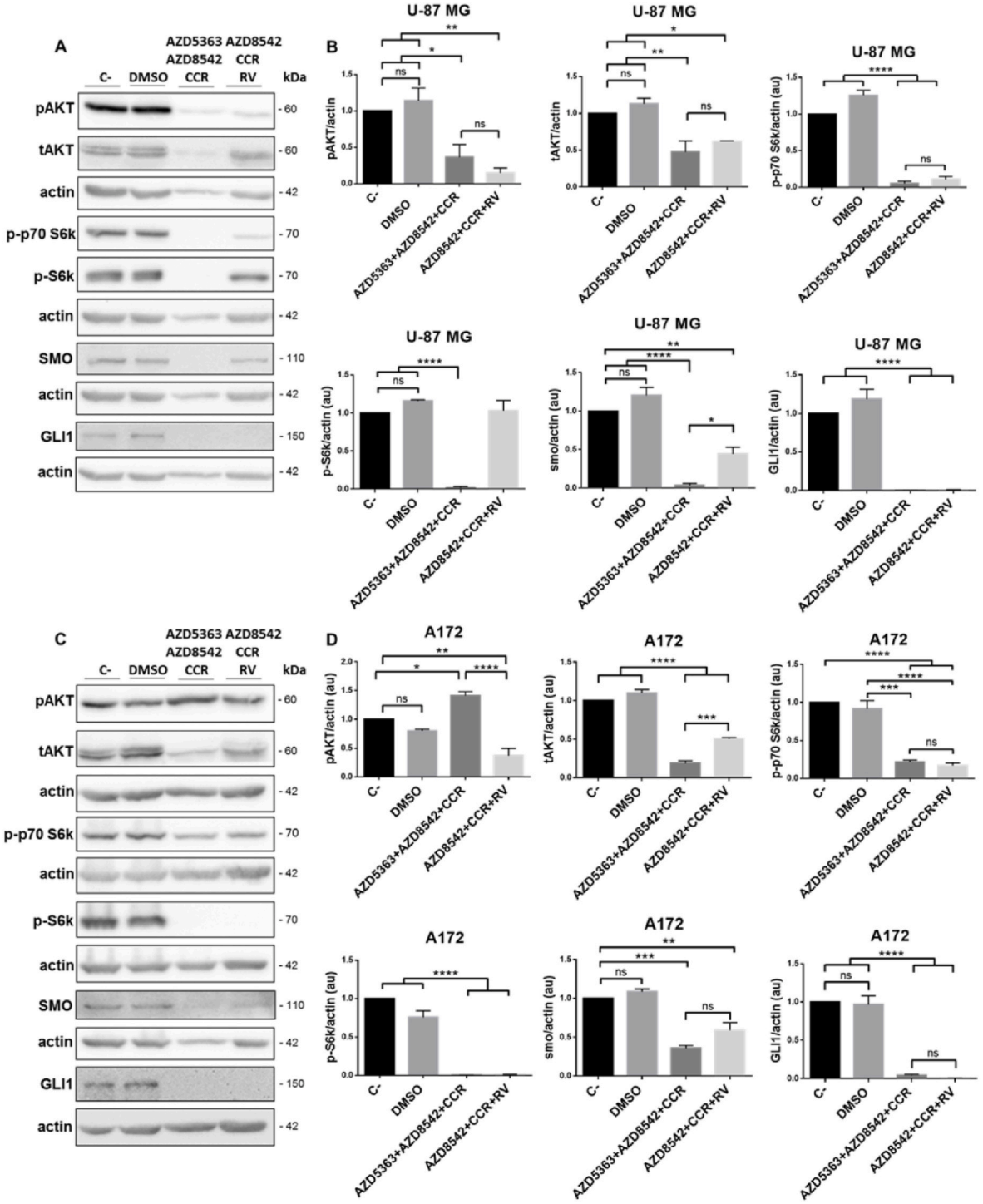

Fig. 5. Effect of the combined treatments with AZD5363+AZD8542+CCR or AZD8542+CCR+RV on the activity of the PI3K/AKT and SHH survival pathways on U-87 MG and A172 cell lines. (A) and (C) representative images of the Western blot analysis of pAKT, tAKT, p-p70 S6k, p-S6k, SMO, GLI1 on U-87 MG (upper panel) and A172 (lower panel), cell lines. (B) and (D) quantitative analysis of the western blots for pAKT, tAKT, p-p70 S6k, p-S6k, SMO, GLI1 on U-87 MG (upper panel) and A172 (lower panel) cells. Data obtained from three independent experiments. Actin was used as loading control. One-way ANOVA, followed by Tukey; *$p < 0.05$, **$p < 0.01$, ***$p < 0.001$, ****$p < 0.0001$. ns, non-significant.

3.6. AZD5363+AZD8542+CCR and AZD8542+CCR+RV induce cell death associated to the activation of caspase-3

p21 is overexpressed in some cancers, and the up-regulation of p21 correlates positively with tumor grade, invasiveness and aggressiveness, and it is a poor prognostic indicator [60]. Frequently, malignant gliomas over-express p21, while oligodendrogliomas and low-grade astrocytomas are p21 negative [61–64]. Moreover, in high-grade astrocytoma, cytoplasmic p27 is associated with a worse prognosis, while nuclear p27 shows a tendency towards a better prognosis [65]. Therefore, we decided to explore the effect of 48 h of treatments on the expression of p21, p27 and ciclyn-D1. We observed, by Western blot analysis, that the expression of both p21 and p27 decreases in the U-87 MG (Fig. 6B) and A172 (Fig. 6D) cell lines when the two combined treatments were compared with the controls. Thus, the combinations AZD5363+AZD8542+CCR and AZD8542+CCR+RV detain the oncogenic activity of p21 and p27. On the other hand, it was observed, by Western blot analysis, that the expression of ciclyn-D1 decreased in the U-87 MG (Fig. 6B) and A172 (Fig. 6D) cell lines treated with AZD5363+AZD8542+CCR combination, while, with AZD8542+CCR+RV the expression of ciclyn-D1 was preserved. Additionally, we assessed the activation of caspase-3 (cas-3) as a marker of apoptosis. We observed a discrete activation of cas-3, after exposure to AZD8542+CCR+RV in the A172 cell line (Fig. 6D), but more intense effects were observed after exposure to AZD 5363+AZD8542+CCR in the U-87 MG and A172 cell lines and AZD8542+CCR+RV in the U-87 MG cell line (Fig. 6B and D). These data show that the combined treatment with AZD5363+AZD8542+CCR or AZD8542+CCR+RV induce an apoptotic process in the U-87 MG and A172 cell lines.

In summary, the administration of the combined treatments AZD5363+AZD8542+CCR or AZD8542+CCR+RV inhibit the proliferation and induce cell death associated with the apoptosis of human GBM cells (Fig. 7).

4. Discussion

In the present study, we used AZD5363, AZD8542, CCR and RV to treat GBM and obtained interesting results *in vitro*, however it is necessary to evaluate their effects in non-cancerous cells *in vitro* and *in vivo* to rule out cytotoxicity in the body and to analyze the body's metabolic response.

CCR and RV have recently been classified as PAINS (pan assay interference compounds), these compounds have false activity against a wide variety of molecular targets, the false activity of CCR and RV in multiple assays may be due to the use of non-pure mixtures of these compounds, leading to a response against multiple targets [28,66]. Moreover, CCR and RV have been reported to have limited biological activity due to low oral bioavailability, even through intraveneous administration [67–70] however, there are different pharmaceutical strategies that can improve the bioavailability of CCR and RV including enhancing agents [71], nanoparticles [72,73], phospholipid complex [74], liposomes [75,76], solid dispersions [77,78] and microemulsifying [79]. On the other hand, both CCR and RV are chemically unstable molecules, a fact that complicates their study; however, there are strategies that can avoid their chemical instability, such as the use of lipids or nanoparticles [28]. Despite some of the characteristics previously mentioned, the information obtained in this study, together with an ample body of research indicate, that treatments including the use of CCR and RV, could be useful for the development of possible alternative therapeutic strategies against GBM. Considering the properties of CCR and RV, we believe that the present results provide an interesting approach of the potential of the proposed treatments, the data presented here were all obtained *in vitro*, thus future studies in whole animal will be necessary to determine its efficacy and safety.

Recent experimental strategies designed to increase the efficacy of treatments against cancer include combined therapies using two or more agents plus conventional treatments such as chemotherapy, radiotherapy, and surgery. Combination of biologically active agents with mutually interdependent activities is a relevant strategy to block different cellular targets involved in cancer development simultaneously to induce the death of cancer cells. Moreover, combined therapy reduces drug-resistance, toxic effects and has many benefits as it decreases the time of treatment and the use of natural products, compared with monotherapy [54]. In this work, we observed that the combined treatments are more effective decreasing cell survival than any of the agents when applied independently (Fig. 2). Of the eleven combinations tested, the most effective in both cell lines were AZD5363+AZD8542+CCR, AZD5363+AZD8542+RV or AZD8542+CCR+RV, suggesting that the compounds associated with these combinations are complementary and contribute to induce a better effect. The combination of the four agents was not significantly different compared with the combination of three agents. Therefore, we decided to discard the AZD5363+AZD8542+CCR+RV combination. The combined treatments have other therapeutic properties. [80]. Subsequently, the effects of these combined therapies could be evaluated in non-cancerous controls, in order to have an approximation of what would happen in healthy tissue; this information will reinforce the therapeutic potential of this pharmacological strategy.

Previous studies have shown that when an anticancer agent is withdrawn, a few cancer cells survive and may eventually resume division and continue proliferating [81–83]. In addition, some drug-treated cancer cells undergo prolonged growth arrest but do not die [84]. Taken together, these results indicate that some anticancer agents are not effective achieving a long-term effect. Thus, we used clonogenic assays to determine the efficacy of the combined treatments on the capacity of surviving single cells to generate colonies. We observed that combined treatments of AZD5363+AZD8542+CCR and AZD8542+CCR+RV did not permit the formation of colonies, therefore these treatments could reduce the probability of cancer recurrence (Fig. 3C). In this regard, we observed a drastic decrease in cell proliferation during the first 24 h of culture (Fig. 4B), this suggests that after 24 h of treatment the cells are irreversibly damaged, these data are in agreement with the clonogenic assay. On the other hand, GBM has a heterogeneous cellular composition that includes a small subpopulation of cancer stem cells (CSCs) which promote tumor initiation and resistance to chemotherapy and radiotherapy, hence contributing to tumor progression and recurrence. Thus, we employed gliomaspheres, a well-established model of GBM stem-like cells [44,85–87]. Our results suggest a potential therapeutic strategy to reduce the recurrence of GBM.

The combination of AZD5363+AZD8542+CCR or AZD8542+CCR+RV maintain or even increased the expression of AKT in U-87 MG and A-172 cells, however downstream effectors of the AKT like p-p70 S6k and p-S6k, are reduced. These results are consistent with data obtained in other cell lines, for instance the phosphorylation of AKT is increased in PC3, DU145, LNCaP prostate cancer cells and in BT474 breast cancer cells and meningioma cells, after being treated with AZD5363, an ATP-competitive AKT inhibitor [15,88,89]. CCR and RV are also AKT kinase inhibitors and can bind to its catalytic site [14,90,91]. Upon AKT recruitment to the plasma membrane, it adopts an active conformation, exposing the ATP binding pocket and permits access to the regulatory kinases that phosphorylate AKT regulatory residues Ser-473 and Thr-308 [92–94]. When an ATP-competitive AKT inhibitor binds to the catalytic site, it permits an accumulation of inactive and highly phosphorylated AKT bound to the plasma membrane, which prevents the interaction with the PP2A and PHLPP1 phosphatases, thus maintaining stable levels of phosphorylated AKT [95]. It has been reported that ATP-competitive AKT inhibitors cause aberrant AKT phosphorylation on the AKT regulatory residues and that they also reduce the phosphorylation of AKT downstream targets such as GSK3α/β, FOXO3 and S6k, therefore, inhibiting the growth of cancer cells *in vitro*, and tumor growth in xenograft animal models [83,96,97]. On the other

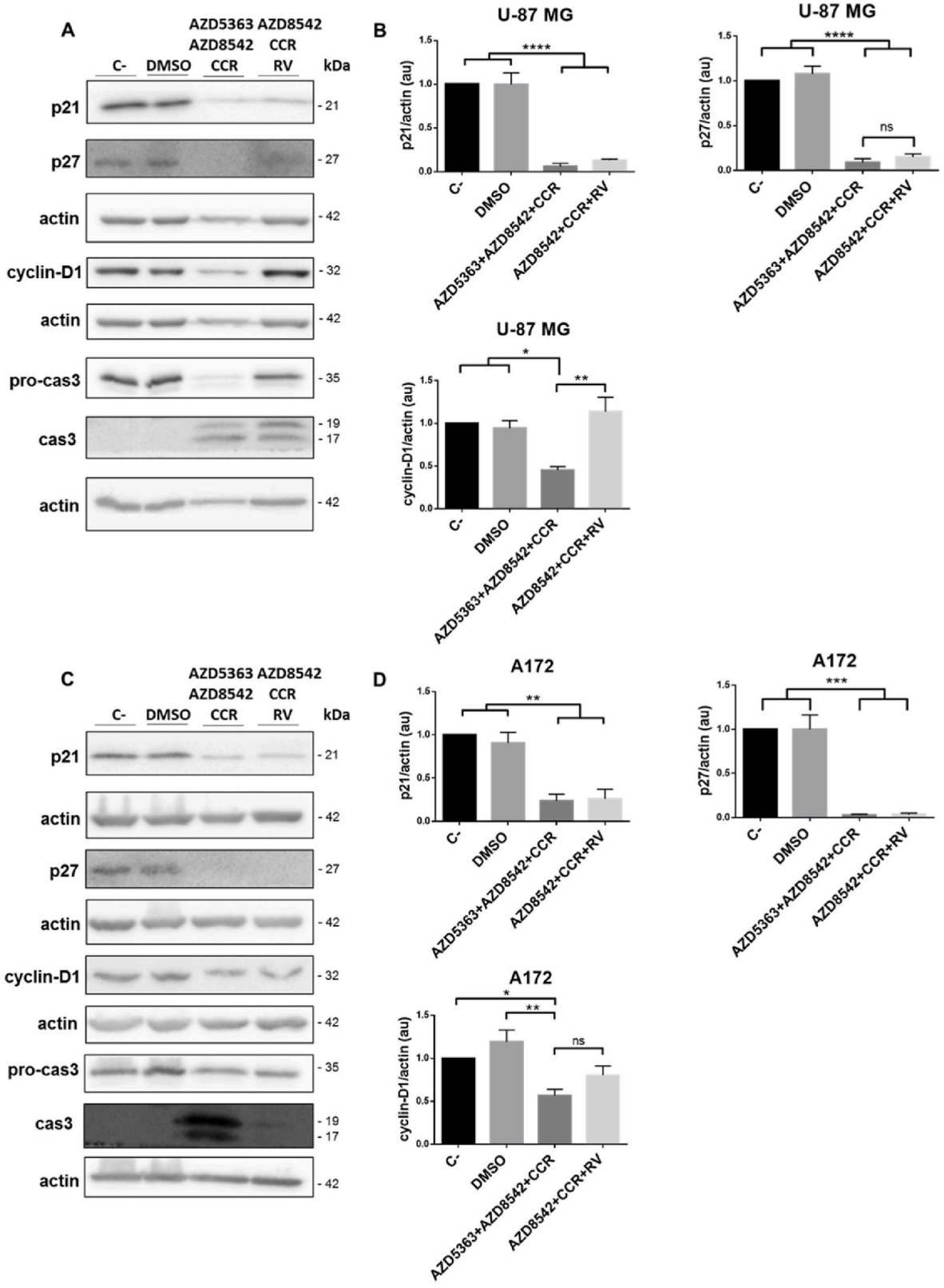

Fig. 6. Effect of the combined treatments with AZD5363+AZD8542+CCR or AZD8542+CCR+RV on the cell-cycle and caspase-dependent apoptosis on U-87 MG and A172 cell lines. (A) and (C) are representative images of the Western blot analysis of p21, p27, cyclin-D1, procas-3 and cas-3 on U-87 MG (upper panel) and A172 (lower panel), cell lines. (B) and (D) quantitative analysis of the western blots for p21, p27, cyclin-D1, procas-3 and cas-3 on U-87 MG (upper panel) and A172 (lower panel) cells. Data obtained from three independent experiments. Actin was used as loading control. Statistical analysis was performed using One-way ANOVA, followed by Tukey. Statistical significance levels are indicated as: *$p < 0.05$, **$p < 0.01$, ***$p < 0.001$, ****$p < 0.0001$. ns, non-significant.

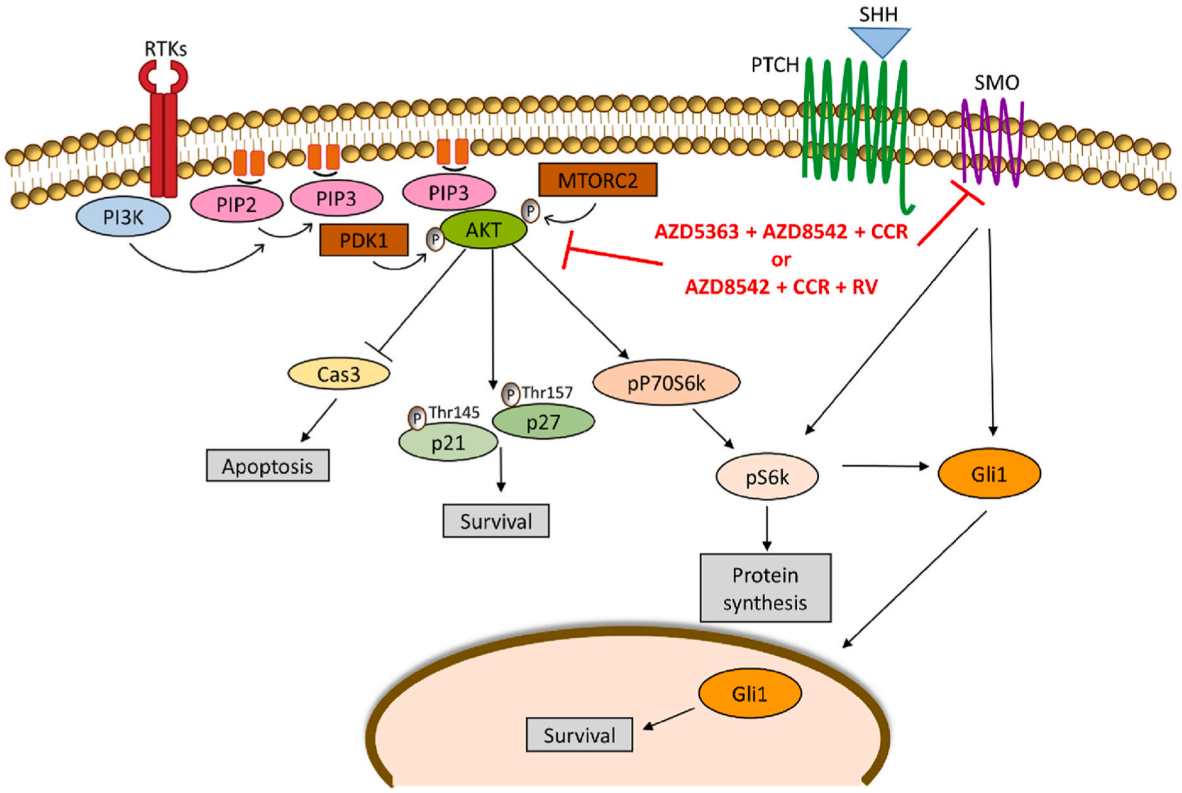

Fig. 7. Proposed model to explain the action of the combined treatments. The combined treatments AZD5363+AZD8542+CCR or AZD8542+CCR+RV decrease the activation of AKT, reduce the expression of SMO, pP70S6k, pS6k, GLI1, p21 and p27, and activate the caspase-3 on U-87 MG and A172 cell lines.

hand, it was previously demonstrated that the hyper-phosphorylation of AKT induced by an ATP-competitive inhibitor renders the AKT enzyme extremely active after removing the inhibitor from the culture medium, suggesting it could promote oncogenesis [97]. In this regard, it is noteworthy that in the colony formation assays, we observed that after removing the AZD5363+AZD8542+CCR mix or the AZD 8542+CCR+RV combination from the culture medium, neither the U-87 MG nor the A172 cells survive, despite the fact that according to western blotting we observed aberrant levels of phosphorylated AKT, these observations suggest the combinations could cause irreversible damage to the cells, this, however, will have to be evaluated in animal models to determine if there is a long-term effect.

On the other hand, the growth-inhibitory activity of p21 is associated with its nuclear localization, since, cytoplasmic p21 promotes cellular proliferation and has anti-apoptotic activity [60,98,99] by inhibiting proteins involved in apoptosis, including procaspase-3, caspase-8, caspase-10 and the assembly of D-type cyclins (D1, D2 and D3) with CDK4 and CDK6. Moreover, p21 also suppresses genes such as *MYC* and *E2F1* which are factors with anti-apoptotic activities [99]. These data coincide with our results, because we observed that in the U-87 MG and A172 cells treated with AZD5363+AZD8542+CCR or AZD536 3+AZD8542+RV, the expression of p21 and p27 decreased and caspase-3 was activated (Fig. 6). Furthermore, AKT phosphorylates p21 on Thr-145 and p27 on Thr-157 so that they remain in the cytoplasm. When AKT is blocked, p21 and p27 lose their oncogenic activity [100–103]. We observed a marked decrease in the expression of both p21 and p27, thus, we suggest that AKT may contribute to tumor cell proliferation by phosphorylating and retaining p21 and p27 in the cytosol. This prevents the inhibition triggered by CDKs. p21 and p27, promote the assembly of cdk4/cyclin-D1 complexes, and a direct interaction is necessary between the kinase and the cyclin, hence, in the absence of p21 and p27 most of the complex is dissociated and there is minimal kinase activity, while in their presence nearly all of the complex remains intact [104]. In this regard, it is most likely that in the U-87 MG and A172 cells receiving the combination treatments AZD 5363+AZD8542+CCR or AZD5363+AZD8542+RV, the cdk4/cyclin-D1 complex is dissociated by the absence of p21 and p27 and cell proliferation is prevented despite the fact that we observed a discrete decrease in the expression of cyclin-D1 (Fig. 6). The Edu assay corroborates these findings, since they show that the proliferation decreases markedly in the U-87 MG and A172 cells after 24 h with the combined treatments (Fig. 4C).

A model of the mechanism proposed is shown in Fig. 7. The therapeutic strategy of employing combined administration of AZD5363, AZD8542, CCR and RV in human GBM cells, shows that combined treatments are potential anti-tumoral strategies. In this case, the combinations AZD5363+AZD8542+CCR and AZD5363+AZD8542+RV, reduced the proliferation and induce apoptosis, by interfering with the activation of PI3K/AKT and SHH survival pathways, the regulation of p21 and p27 and the activation of caspase-3. These results strongly suggest that it is worthwhile to further investigate the use of combined therapies to counteract this cancer.

Declaration of interests

The authors declare that they have no known competing financial interests or personal relationships that could have appeared to influence the work reported in this paper.

Data availability

Data will be made available on request.

Acknowledgements

This work was partially support by Conacyt (México) grant 1563

Fronteras de la Ciencia (JS); RMR received a scholarship (275144) from Conacyt. We thank AstraZeneca for the kind gift of the AZD5363 and AZD8542 compounds.

Appendix A. Supplementary data

Supplementary data to this article can be found online at https://doi.org/10.1016/j.bbrep.2023.101430.

References

[1] G. Reifenberger, et al., Pathology and Classifi cation of Tumors of the Nervous System, Oncol. CNS Tumors (2010) 3–75.
[2] F.B. Furnari, et al., Malignant astrocytic glioma: genetics, biology, and paths to treatment, Genes Dev. 21 (21) (2007) 2683–2710.
[3] E.A. Maher, et al., Malignant glioma: genetics and biology of a grave matter, Genes Dev. 15 (11) (2001) 1311–1333.
[4] Q.T. Ostrom, et al., CBTRUS statistical report: primary brain and other central nervous system tumors diagnosed in the United States in 2012-2016, Neuro Oncol. 21 (5) (2019) v1–v100.
[5] M. Nakada, et al., Aberrant signaling pathways in glioma, Cancers 3 (3) (2011) 3242–3278.
[6] S. Godard, et al., Classification of human astrocytic gliomas on the basis of gene expression: a correlated group of genes with angiogenic activity emerges as a strong predictor of subtypes, Cancer Res. 63 (20) (2003) 6613–6625.
[7] N. Cancer Genome Atlas Research, Comprehensive genomic characterization defines human glioblastoma genes and core pathways, Nature 455 (7216) (2008) 1061–1068.
[8] A.B.-Y. Hui, et al., Detection of multiple gene amplifications in glioblastoma multiforme using array-based comparative genomic hybridization, Lab. Invest. vol. 81 (2001) 717–723.
[9] A. Chakravarti, et al., The prognostic significance of phosphatidylinositol 3-kinase pathway activation in human gliomas, J. Clin. Oncol. 22 (10) (2004) 1926–1933.
[10] Y. Ruano, et al., Identification of survival-related genes of the phosphatidylinositol 3'-kinase signaling pathway in glioblastoma multiforme, Cancer 112 (7) (2008) 1575–1584.
[11] H. Mure, et al., Akt2 and Akt3 play a pivotal role in malignant gliomas, Neuro Oncol. 12 (3) (2010) 221–232.
[12] C. Wetmore, Sonic hedgehog in normal and neoplastic proliferation: insight gained from human tumors and animal models, Curr. Opin. Genet. Dev. 13 (1) (2003) 34–42.
[13] V. Clement, et al., HEDGEHOG-GLI1 signaling regulates human glioma growth, cancer stem cell self-renewal, and tumorigenicity, Curr. Biol. 17 (2) (2007) 165–172.
[14] M. Addie, et al., Discovery of 4-amino-N-[(1S)-1-(4-chlorophenyl)-3-hydroxypropyl]-1-(7H-pyrrolo[2,3-d]pyrimidin -4-yl)piperidine-4-carboxamide (AZD5363), an orally bioavailable, potent inhibitor of Akt kinases, J. Med. Chem. 56 (5) (2013) 2059–2073.
[15] P. John, et al., AKT1(E17K) -mutated meningioma cell lines respond to treatment with the AKT inhibitor AZD5363, Neuropathol. Appl. Neurobiol. 48 (2) (2022), e12780.
[16] R.F. Hwang, et al., Inhibition of the hedgehog pathway targets the tumor-associated stroma in pancreatic cancer, Mol. Cancer Res. 10 (9) (2012) 1147–1157.
[17] S.C. Gupta, S. Patchva, B.B. Aggarwal, Therapeutic roles of curcumin: lessons learned from clinical trials, AAPS J. 15 (1) (2013) 195–218.
[18] S. Purkayastha, et al., Curcumin blocks brain tumor formation, Brain Res. 1266 (2009) 130–138.
[19] W.Z. Du, et al., Curcumin suppresses malignant glioma cells growth and induces apoptosis by inhibition of SHH/GLI1 signaling pathway in vitro and vivo, CNS Neurosci. Ther. 19 (12) (2013) 926–936.
[20] X. Wang, et al., Curcumin exerts its tumor suppressive function via inhibition of NEDD4 oncoprotein in glioma cancer cells, Int. J. Oncol. 51 (2) (2017) 467–477.
[21] S. Karmakar, et al., Curcumin activated both receptor-mediated and mitochondria-mediated proteolytic pathways for apoptosis in human glioblastoma T98G cells, Neurosci. Lett. 407 (1) (2006) 53–58.
[22] A. Zanotto-Filho, et al., The curry spice curcumin selectively inhibits cancer cells growth in vitro and in preclinical model of glioblastoma, J. Nutr. Biochem. 23 (6) (2012) 591–601.
[23] A. Mukhopadhyay, et al., Curcumin downregulates cell survival mechanisms in human prostate cancer cell lines, Oncogene 20 (52) (2001) 7597–7609.
[24] K. Mehta, et al., Antiproliferative effect of curcumin (diferuloylmethane) against human breast tumor cell lines, Anti Cancer Drugs 8 (5) (1997) 470–481.
[25] S. Yin, et al., MicroRNA-326 sensitizes human glioblastoma cells to curcumin via the SHH/GLI1 signaling pathway, Cancer Biol. Ther. 19 (4) (2018) 260–270.
[26] J. Zhao, et al., Curcumin potentiates the potent antitumor activity of ACNU against glioblastoma by suppressing the PI3K/AKT and NF-kappaB/COX-2 signaling pathways, OncoTargets Ther. 10 (2017) 5471–5482.
[27] R. Jagannathan, P.M. Abraham, P. Poddar, Temperature-dependent spectroscopic evidences of curcumin in aqueous medium: a mechanistic study of its solubility and stability, J. Phys. Chem. B 116 (50) (2012) 14533–14540.
[28] K.M. Nelson, et al., The essential medicinal chemistry of curcumin, J. Med. Chem. 60 (5) (2017) 1620–1637.
[29] Y.J. Wang, et al., Stability of curcumin in buffer solutions and characterization of its degradation products, J. Pharm. Biomed. Anal. 15 (12) (1997) 1867–1876.
[30] J. Burns, et al., Plant foods and herbal sources of resveratrol, J. Agric. Food Chem. 50 (11) (2002) 3337–3340.
[31] A. Shrikanta, A. Kumar, V. Govindaswamy, Resveratrol content and antioxidant properties of underutilized fruits, J. Food Sci. Technol. 52 (1) (2015) 383–390.
[32] L.G. Carter, J.A. D'Orazio, K.J. Pearson, Resveratrol and cancer: focus on in vivo evidence, Endocr. Relat. Cancer 21 (3) (2014) R209–R225.
[33] S. Sheth, et al., Resveratrol reduces prostate cancer growth and metastasis by inhibiting the Akt/MicroRNA-21 pathway, PLoS One 7 (12) (2012), e51655.
[34] S. Yang, et al., Resveratrol elicits anti-colorectal cancer effect by activating miR-34c-KITLG in vitro and in vivo, BMC Cancer 15 (2015) 969.
[35] P.A. Clark, et al., Resveratrol targeting of AKT and p53 in glioblastoma and glioblastoma stem-like cells to suppress growth and infiltration, J. Neurosurg. 126 (5) (2017) 1448–1460.
[36] L. Le Corre, et al., Resveratrol and breast cancer chemoprevention: molecular mechanisms, Mol. Nutr. Food Res. 49 (5) (2005) 462–471.
[37] Q. Gao, et al., Resveratrol inhibits the hedgehog signaling pathway and epithelial-mesenchymal transition and suppresses gastric cancer invasion and metastasis, Oncol. Lett. 9 (5) (2015) 2381–2387.
[38] A. Slusarz, et al., Common botanical compounds inhibit the hedgehog signaling pathway in prostate cancer, Cancer Res. 70 (8) (2010) 3382–3390.
[39] Q. Wang, et al., Resveratrol protects against global cerebral ischemic injury in gerbils, Brain Res. 958 (2) (2002) 439–447.
[40] M. Annaji, et al., Resveratrol-loaded nanomedicines for cancer applications, Cancer Rep (Hoboken) 4 (3) (2021), e1353.
[41] A. Shaito, et al., Potential adverse effects of resveratrol: a literature review, Int. J. Mol. Sci. 21 (6) (2020).
[42] L. Qiang, et al., Isolation and characterization of cancer stem like cells in human glioblastoma cell lines, Cancer Lett. 279 (1) (2009) 13–21.
[43] C.N. Im, et al., BIS-mediated STAT3 stabilization regulates glioblastoma stem cell-like phenotypes, Oncotarget 7 (23) (2016) 35056–35070.
[44] F. Erhart, et al., Gliomasphere marker combinatorics: multidimensional flow cytometry detects CD44+/CD133+/ITGA6+/CD36+ signature, J. Cell Mol. Med. 23 (1) (2019) 281–292.
[45] D. Romero-Trejo, et al., The systemic administration of neural stem cells expressing an inducible and soluble form of growth arrest specific 1 inhibits mammary gland tumor growth and the formation of metastases, Cytotherapy 23 (3) (2021) 223–235.
[46] L. Sanchez-Hernandez, et al., Additive effects of the combined expression of soluble forms of GAS1 and PTEN inhibiting glioblastoma growth, Gene Ther. 25 (6) (2018) 439–449.
[47] Y. Takayama, K. Kusamori, M. Nishikawa, Click chemistry as a tool for cell engineering and drug delivery, Molecules 24 (1) (2019).
[48] L. Daniel-Garcia, et al., Simultaneous treatment with soluble forms of GAS1 and PTEN reduces invasiveness and induces death of pancreatic cancer cells, OncoTargets Ther. 13 (2020) 11769–11779.
[49] H.S. Phillips, et al., Molecular subclasses of high-grade glioma predict prognosis, delineate a pattern of disease progression, and resemble stages in neurogenesis, Cancer Cell 9 (3) (2006) 157–173.
[50] K.W. Kinzler, et al., Identification of an amplified, highly expressed gene in a human glioma, Science 236 (4797) (1987) 70–73.
[51] O.J. Becher, et al., Gli activity correlates with tumor grade in platelet-derived growth factor-induced gliomas, Cancer Res. 68 (7) (2008) 2241–2249.
[52] W. Du, et al., Targeting the SMO oncogene by miR-326 inhibits glioma biological behaviors and stemness, Neuro Oncol. 17 (2) (2015) 243–253.
[53] D. Hanahan, R.A. Weinberg, Hallmarks of cancer: the next generation, Cell 144 (5) (2011) 646–674.
[54] R. Bayat Mokhtari, et al., Combination therapy in combating cancer, Oncotarget 8 (23) (2017) 38022–38043.
[55] T.A. Yap, A. Omlin, J.S. de Bono, Development of therapeutic combinations targeting major cancer signaling pathways, J. Clin. Oncol. 31 (12) (2013) 1592–1605.
[56] M. Weller, et al., Standards of care for treatment of recurrent glioblastoma–are we there yet? Neuro Oncol. 15 (1) (2013) 4–27.
[57] N.A. Franken, et al., Clonogenic assay of cells in vitro, Nat. Protoc. 1 (5) (2006) 2315–2319.
[58] M.G. Filbin, et al., Coordinate activation of Shh and PI3K signaling in PTEN-deficient glioblastoma: new therapeutic opportunities, Nat. Med. 19 (11) (2013) 1518–1523.
[59] L. Chang, et al., [Corrigendum] Activation of sonic hedgehog signaling enhances cell migration and invasion by induction of matrix metalloproteinase-2 and -9 via the phosphoinositide-3 kinase/AKT signaling pathway in glioblastoma, Mol. Med. Rep. 12 (5) (2015) 7815.
[60] T. Abbas, A. Dutta, p21 in cancer: intricate networks and multiple activities, Nat. Rev. Cancer 9 (6) (2009) 400–414.
[61] T. Kokunai, et al., Overcoming of radioresistance in human gliomas by p21WAF1/CIP1 antisense oligonucleotide, J. Neuro Oncol. 51 (2) (2001) 111–119.
[62] P. Korkolopoulou, et al., Expression of retinoblastoma gene product and p21 (WAF1/Cip 1) protein in gliomas: correlations with proliferation markers, p53 expression and survival, Acta Neuropathol. 95 (6) (1998) 617–624.
[63] T. Kokunai, N. Tamaki, Relationship between expression of p21WAF1/CIP1 and radioresistance in human gliomas, Jpn. J. Cancer Res. 90 (6) (1999) 638–646.

[64] J.M. Jung, et al., Increased levels of p21WAF1/Cip1 in human brain tumors, Oncogene 11 (10) (1995) 2021–2028.
[65] T. Hidaka, et al., The combination of low cytoplasmic and high nuclear expression of p27 predicts a better prognosis in high-grade astrocytoma, Anticancer Res. 29 (2) (2009) 597–603.
[66] O. Vang, Resveratrol: challenges in analyzing its biological effects, Ann. N. Y. Acad. Sci. 1348 (1) (2015) 161–170.
[67] V.S. Ipar, A. Dsouza, P.V. Devarajan, Enhancing curcumin oral bioavailability through nanoformulations, Eur. J. Drug Metab. Pharmacokinet. 44 (4) (2019) 459–480.
[68] Z. Ma, et al., Pharmaceutical strategies of improving oral systemic bioavailability of curcumin for clinical application, J. Contr. Release 316 (2019) 359–380.
[69] S. Galiniak, D. Aebisher, D. Bartusik-Aebisher, Health benefits of resveratrol administration, Acta Biochim. Pol. 66 (1) (2019) 13–21.
[70] A. Chimento, et al., Progress to improve oral bioavailability and beneficial effects of resveratrol, Int. J. Mol. Sci. 20 (6) (2019).
[71] G. Shoba, et al., Influence of piperine on the pharmacokinetics of curcumin in animals and human volunteers, Planta Med. 64 (4) (1998) 353–356.
[72] X. Xie, et al., PLGA nanoparticles improve the oral bioavailability of curcumin in rats: characterizations and mechanisms, J. Agric. Food Chem. 59 (17) (2011) 9280–9289.
[73] E.H. Gokce, et al., Resveratrol-loaded solid lipid nanoparticles versus nanostructured lipid carriers: evaluation of antioxidant potential for dermal applications, Int. J. Nanomed. 7 (2012) 1841–1850.
[74] K. Maiti, et al., Curcumin-phospholipid complex: preparation, therapeutic evaluation and pharmacokinetic study in rats, Int. J. Pharm. 330 (1–2) (2007) 155–163.
[75] A. Kunwar, et al., Transport of liposomal and albumin loaded curcumin to living cells: an absorption and fluorescence spectroscopic study, Biochim. Biophys. Acta 1760 (10) (2006) 1513–1520.
[76] A.R. Neves, et al., Novel resveratrol nanodelivery systems based on lipid nanoparticles to enhance its oral bioavailability, Int. J. Nanomed. 8 (2013) 177–187.
[77] C.W. Chang, et al., Development of a solid dispersion system for improving the oral bioavailability of resveratrol in rats, Eur. J. Drug Metab. Pharmacokinet. 42 (2) (2017) 239–249.
[78] S.W. Seo, et al., Preparation and pharmacokinetic evaluation of curcumin solid dispersion using Solutol(R) HS15 as a carrier, Int. J. Pharm. 424 (1–2) (2012) 18–25.
[79] F.F. Yang, et al., Improving oral bioavailability of resveratrol by a UDP-glucuronosyltransferase inhibitory excipient-based self-microemulsion, Eur. J. Pharmaceut. Sci. 114 (2018) 303–309.
[80] R. Vengoji, et al., Natural products: a hope for glioblastoma patients, Oncotarget 9 (31) (2018) 22194–22219.
[81] C. Demarcq, et al., The role of cell cycle progression in cisplatin-induced apoptosis in Chinese hamster ovary cells, Cell Growth Differ. 5 (9) (1994) 983–993.
[82] A.L. Kung, et al., Cytotoxic effects of cell cycle phase specific agents: result of cell cycle perturbation, Cancer Res. 50 (22) (1990) 7307–7317.
[83] Y. Luo, et al., Potent and selective inhibitors of Akt kinases slow the progress of tumors in vivo, Mol. Cancer Therapeut. 4 (6) (2005) 977–986.
[84] B.D. Chang, et al., A senescence-like phenotype distinguishes tumor cells that undergo terminal proliferation arrest after exposure to anticancer agents, Cancer Res. 59 (15) (1999) 3761–3767.
[85] J.D. Lathia, et al., Cancer stem cells in glioblastoma, Genes Dev. 29 (12) (2015) 1203–1217.
[86] J. Chen, et al., A restricted cell population propagates glioblastoma growth after chemotherapy, Nature 488 (7412) (2012) 522–526.
[87] S. Bao, et al., Glioma stem cells promote radioresistance by preferential activation of the DNA damage response, Nature 444 (7120) (2006) 756–760.
[88] F. Lamoureux, et al., Blocked autophagy using lysosomotropic agents sensitizes resistant prostate tumor cells to the novel Akt inhibitor AZD5363, Clin. Cancer Res. 19 (4) (2013) 833–844.
[89] B.R. Davies, et al., Preclinical pharmacology of AZD5363, an inhibitor of AKT: pharmacodynamics, antitumor activity, and correlation of monotherapy activity with genetic background, Mol. Cancer Therapeut. 11 (4) (2012) 873–887.
[90] V. Vishwakarma, et al., Potent antitumor effects of a combination of three nutraceutical compounds, Sci. Rep. 8 (1) (2018), 12163.
[91] T.C. Hsieh, et al., Biochemical and cellular evidence demonstrating AKT-1 as a binding partner for resveratrol targeting protein NQO2, PLoS One 9 (6) (2014), e101070.
[92] C.C. Kumar, V. Madison, AKT crystal structure and AKT-specific inhibitors, Oncogene 24 (50) (2005) 7493–7501.
[93] J.Q. Cheng, et al., The Akt/PKB pathway: molecular target for cancer drug discovery, Oncogene 24 (50) (2005) 7482–7492.
[94] G. Lazaro, E. Kostaras, I. Vivanco, Inhibitors in AKTion: ATP-competitive vs allosteric, Biochem. Soc. Trans. 48 (3) (2020) 933–943.
[95] T.O. Chan, et al., Resistance of Akt kinases to dephosphorylation through ATP-dependent conformational plasticity, Proc. Natl. Acad. Sci. U. S. A. 108 (46) (2011) E1120–E1127.
[96] E.K. Han, et al., Akt inhibitor A-443654 induces rapid Akt Ser-473 phosphorylation independent of mTORC1 inhibition, Oncogene 26 (38) (2007) 5655–5661.
[97] T. Okuzumi, et al., Inhibitor hijacking of Akt activation, Nat. Chem. Biol. 5 (7) (2009) 484–493.
[98] A. Suzuki, et al., Resistance to Fas-mediated apoptosis: activation of caspase 3 is regulated by cell cycle regulator p21WAF1 and IAP gene family ILP, Oncogene 17 (8) (1998) 931–939.
[99] G.P. Dotto, p21(WAF1/Cip1): more than a break to the cell cycle? Biochim. Biophys. Acta 1471 (1) (2000) M43–M56.
[100] B.P. Zhou, et al., Cytoplasmic localization of p21Cip1/WAF1 by Akt-induced phosphorylation in HER-2/neu-overexpressing cells, Nat. Cell Biol. 3 (3) (2001) 245–252.
[101] J. Liang, et al., PKB/Akt phosphorylates p27, impairs nuclear import of p27 and opposes p27-mediated G1 arrest, Nat. Med. 8 (10) (2002) 1153–1160.
[102] Y.H. Min, et al., Cytoplasmic mislocalization of p27Kip1 protein is associated with constitutive phosphorylation of Akt or protein kinase B and poor prognosis in acute myelogenous leukemia, Cancer Res. 64 (15) (2004) 5225–5231.
[103] I. Shin, et al., PKB/Akt mediates cell-cycle progression by phosphorylation of p27 (Kip1) at threonine 157 and modulation of its cellular localization, Nat. Med. 8 (10) (2002) 1145–1152.
[104] J. LaBaer, et al., New functional activities for the p21 family of CDK inhibitors, Genes Dev. 11 (7) (1997) 847–862.